Pressure-Induced Superconductivity in Topological Materials

Sergey Medvedev[#], KeYuan Ma, Qing-Ge Mu, Jonathan Noky, Dong Chen, Subhajit Roychowdhury, Walter Schnelle, Chandra Shekhar and Claudia Felser

Superconducting materials with topologically nontrivial electronic structure have attracted much attention owing to their exotic quantum-mechanical properties and diverse potential applications. External pressure can drive topological quantum phase transitions, which offers a means for generating and investigating these phases, elucidating the interplay between different ground states. The realization of superconductivity in topological compounds is regarded as an important step in achieving quantum computing. Here, we map the electronic and structural phase diagrams of topologically nontrivial materials via electronic transport measurements (magnetoresistivity, Hall effect), Raman spectroscopy, and synchrotron x-ray diffraction at high pressures. To gain further insight into these pressure-driven transitions, our studies are accompanied by theoretical calculations of electronic band structures.

Superconductivity and topology are two intriguing phenomena of quantum condensed phases. The former arises from electron pairing and the latter emerges from crystal and atomic orbital symmetry. These symmetries enrich the characteristics of the bands, either as bandgaps or degeneracies between two or more protected bands. Consequently, a fundamental attribute of topological phases is the presence of a gapless state at the boundary (surface or edge). This is related to the topology of the bulk electronic structure and its projection onto the boundary.

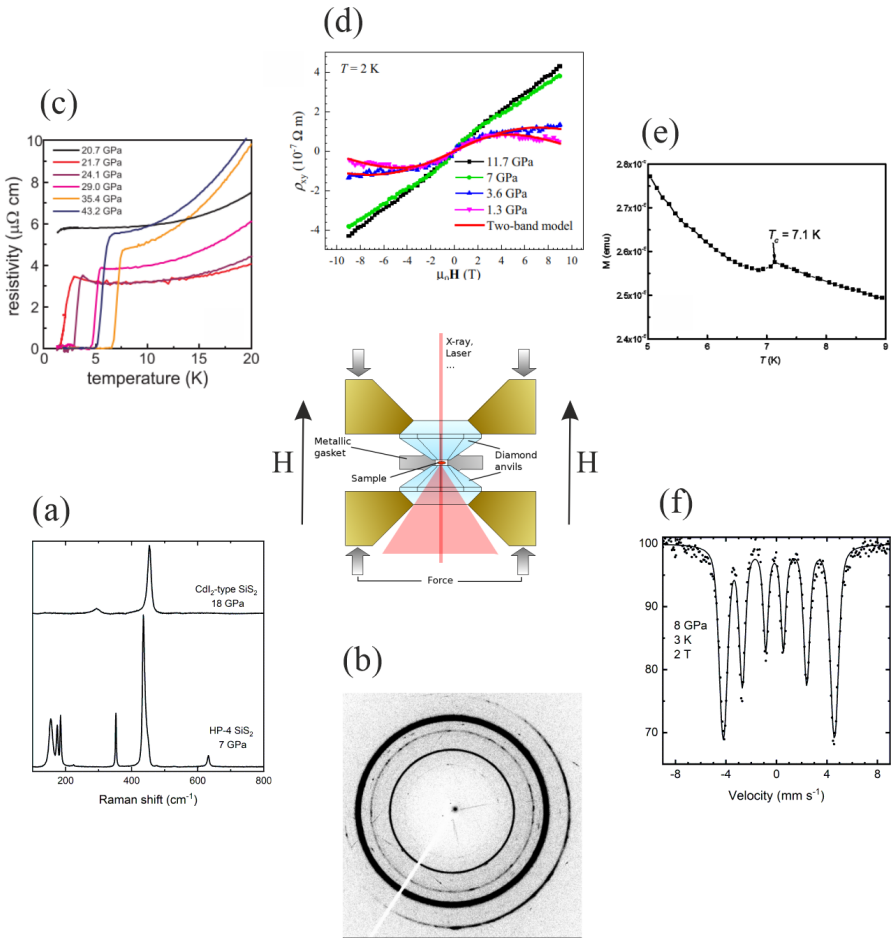

Fig. 1: Schematic of a diamond anvil cell and examples for experimental studies of properties of solids at high pressures: (a) changes in Raman spectra indicating the structural phase transition in SiS_2; [4] (b) synchrotron x-ray powder diffraction pattern of the collapsed tetragonal phase of $BaCr_2As_2$; [5] (c) temperature dependence of the electrical resistivity of PdS_2 in the vicinity of pressure-induced superconducting transition; [6] (d) Nonlinear magnetic field dependence of Hall resistivity of $NbIrTe_4$ at different pressures; [7] (e) magnetization signal of superconducting $MoTe_2$ at 7.5 GPa [8]; (f) synchrotron ^{57}Fe Mössbauer spectra at 8 GPa in magnetic field 2 T. [9]

The combination of superconductivity and topology in a material gives rise to topological superconductivity. These materials can host Majorana fermions, which could have potential applications in quantum computing. Over the past two decades, these aspects have been investigated in several materials. Various Bi-containing topological insulators have been found to be intrinsic superconductors, either by applying chemical pressure and/or doping [1] or by applying external pressure [2]. For example, superconductivity in the topological insulator YPtBi [3] occurs at ambient pressure but seems to extend to unconventional spin-multiplet pairing mechanisms. To better understand new topologically nontrivial phases of matter, it is useful to investigate the competition between different topologically trivial and nontrivial ground states and emerging phenomena by tuning the system via chemical doping or applying a combination of external stimuli such as temperature, magnetic field and pressure. Although high-pressure phases of matter have limited direct applications, performing experiments under pressure is an invaluable tool for discovering and understanding such novel phases. High pressure is a particularly clean method of modifying the crystal structure without introducing chemical impurities or defects.

Although setting up a high-pressure experiment is still difficult and time consuming, studies of the effect of pressure on properties of matter can now be performed using nearly all experimental techniques in temperature ranges from mK to thousands of K and/or at high magnetic fields. To generate pressure up to 100 GPa we have designed our own miniature diamond anvil cells (DAC) schematically shown in Figure 1. The optical transparency of diamond in a wide range of the electromagnetic spectrum allow to perform several spectroscopic methods. Especially, Raman spectroscopy is a powerful method to study the pressure effect on interatomic interactions in the materials, to monitor pressure-induced phase transitions (Figure 1a), and in combination with high-pressure synchrotron x-ray diffraction (Figure 1b), to determine the structures of the new polymorphic forms of compounds [4]. *In situ* measurements of the resistivity of tiny samples with electrical contacts allow to study pressure-induced changes of the electronic properties of matter such as insulator-metal transitions and superconductivity (Figure 1c) [6]. Magnetoresistance and Hall-effect measurements (Figure 1d) are crucial for inferring information about the interactions between itinerant charge carriers and the magnetic degrees of freedom and pressure-induced changes of the electronic structure [7]. Although extremely difficult due to very small volume of the sample in high-pressure experiments, magnetization measurements in SQUIDs (Figure 1e) might be utilized for the observation of the Meissner effect in superconductors at high pressures [8]. The recent development of the synchrotron techniques provides possibilities for detailed studies of the pressure effect on the magnetic ordering by Mössbauer spectroscopy (Figure 1f) in a wide range of pressures, temperatures and applied magnetic fields [9, 10]. Our group is continuously working on the application of new experimental techniques to study the pressure effect on the structural, electronic and magnetic properties of solids. E. g., currently we apply the nuclear forward scattering (NFS) of synchrotron radiation to study the pressure-induced magnetic and valence transitions in Europium-based compounds.

Pressure-induced superconductivity in the weak topological insulator $RhBi_2$

The Bi-rich part of the binary Rh–Bi system has attracted significant interest owing to its superconductivity [11]. Recently, $RhBi_2$ was shown to be a weak topological insulator [12]. $RhBi_2$ is not superconducting at ambient pressure [11]; nevertheless, it exhibits intriguing new physical phenomena under stress or strain.

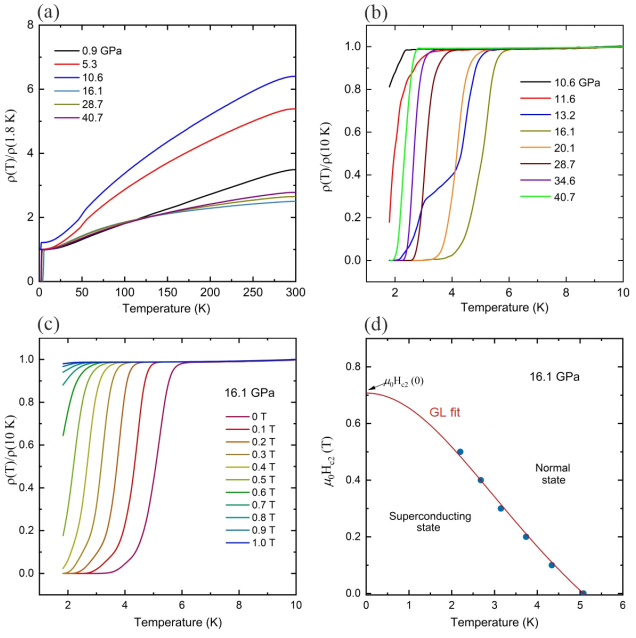

Fig. 2: (a) Temperature dependence of normalized electrical resistivity $\rho/\rho_{1.8\,K}$ for α-$RhBi_2$ at different pressures. (b) Temperature dependence of normalized resistivity $\rho/\rho_{10\,K}$ in the vicinity of the superconducting transition temperature. (c) Temperature dependence of $\rho/\rho_{10\,K}$ for different magnetic fields at 16.1 GPa. (d) Temperature dependence of upper critical field $\mu_0 H_{c2}(T)$ and Ginzburg–Landau fitting curve.

We studied the electronic transport properties of $RhBi_2$ at pressures up to ~40 GPa [13]. High-quality single crystals were grown using the Bi-flux method. The monoclinic unit cell parameters ($P2_1/c$ symmetry with lattice parameters a = 6.9241(13) Å, b = 6.7946(8) Å, c = 6.9587(13) Å and β = 117.73°), as determined by unambiguous indexing of the x-ray diffraction patterns, which agrees with published data for the stable α-phase of $RhBi_2$ at room temperature.

To study the effect of pressure on the electronic properties of α-$RhBi_2$, we measured the temperature dependence of its resistivity at different pressures (Figure 1a). At pressures up to 10.6 GPa, the resistivity decreased monotonously upon cooling, indicating that α-$RhBi_2$ exhibits normal metallic behavior in this pressure range. Superconductivity was not observed in this pressure range upon cooling to 1.8 K (the minimum temperature of the experiment), in accordance with ambient pressure data on $RhBi_2$ [11].

Upon increasing the pressure to 10.6 GPa, an abrupt drop in resistivity was observed at 2 K. This indicates the onset of a superconducting transition (Figure 2a). Indeed, as the pressure was increased to 13.2 GPa, zero resistivity was observed (Figure 2b). The superconducting state was further characterized by a series of resistivity measurements under an applied magnetic field (Figure 2c). The superconducting transition temperature T_c decreased with increasing magnetic field. Notably, at $\mu_0 H$ = 1 T, T_c dropped below our lowest measurement temperature (1.9 K). Fitting the $H_{c2}(T)$ data using the Ginzburg–Landau equation yields an upper critical field $\mu_0 H_{c2}(0)$ = 0.71 T for α-$RhBi_2$ at 16.1 GPa (Figure 2d).

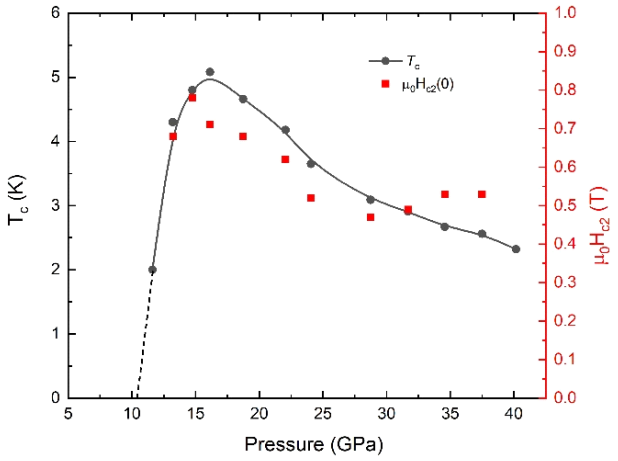

Fig. 3: Pressure dependence of the critical temperature T_c of superconductivity (left axis) and upper critical field $\mu_0 H_{c2}(0)$ (right axis) for α-$RhBi_2$.

In the absence of experimental data on the structural evolution of $RhBi_2$ under pressure, the dynamical stability of α-$RhBi_2$ under compression was examined by calculating the phonon spectrum of the monoclinic α-$RhBi_2$ structure at pressures of up to 40 GPa. Structural stability was observed over the full pressure range, as is indicated by the absence of imaginary phonon modes and a progressive hardening of the acoustical modes with increasing compression [13].

The pressure evolution of the superconducting transition in α-$RhBi_2$ was further studied by measuring the resistivity at pressures up to 40.7 GPa (Figure 2b). T_c rapidly increased with increasing pressure up to 16.1 GPa (T_c = 5.1 K), and then decreased gradually as the pressure increased further, reaching 2.3 K at 40.7 GPa (the highest pressure in this experiment).

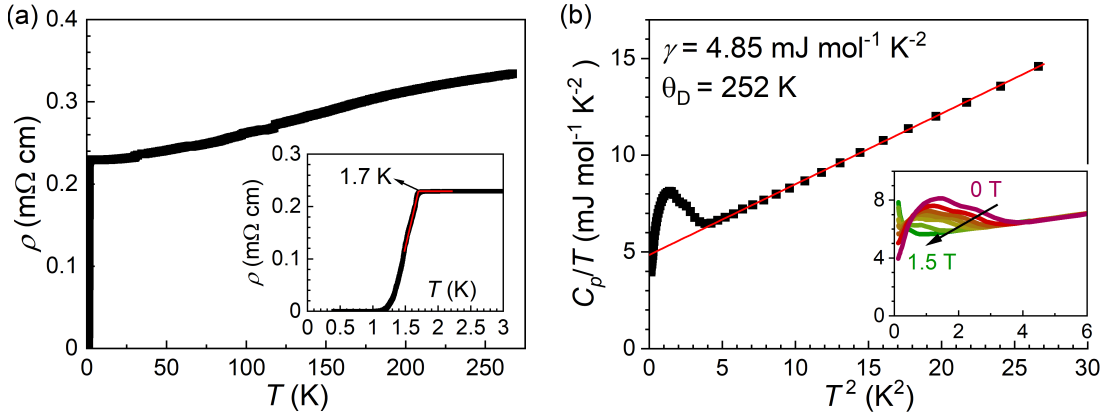

Fig. 4: Superconductivity of $IrBi_{0.8}Te_{1.2}$ at ambient pressure. (a) Metallic conduction behavior is evidenced by the decrease in resistivity upon cooling. Inset: Superconducting transition at low temperature. (b) The heat capacity (shown as C_p/T vs. T^2) exhibits a jump at the superconducting transition temperature, indicating bulk superconductivity. The Sommerfeld parameter and initial Debye temperature are derived from a fit (red line). Inset: Field dependence of heat capacity. The upturn at low temperatures is due to nuclear contributions.

This results in a dome-shaped dependence of T_c on pressure (Figure 3). As anticipated, the value of the upper critical field $\mu_0 H_{c2}(0)$ decreased gradually with increasing pressure until reaching 0.53 T at 37.5 GPa (Figure 3). At all pressures, $\mu_0 H_{c2}(0)$ remained below the Pauli limit, as observed in numerous metal–Bi binary superconducting compounds, including KBi_2, $RbBi_2$, and β-$PdBi_2$.

Our *ab initio* calculations of the band structure revealed a correlation between the dome-shaped dependence of T_c on pressure and the non-monotonic shift of the electron energy relative to the Fermi level at specific points of the Brillouin zone [13]. The observation of pressure-induced superconductivity in the weak topological insulator α-$RhBi_2$ may provide a promising platform to study topological superconductivity.

Superconductivity in the ternary pyrite-type compound $IrBi_{1-x}Te_{1+x}$

Compounds with composition TX_2 (where T is a transition metal and X is a chalcogen or pnictogen) with pyrite-type structure have attracted considerable attention owing to their metal–insulator transitions, with various magnetic and electrical phases ranging from antiferromagnetic insulators to superconductors. Notably, several TX_2 compounds have been reported to have topological properties. For example, $PtBi_2$ was predicted to be a Dirac semimetal, and its superconductivity under pressure was confirmed [14]. In addition, via angle-resolved photoemission spectroscopy, it was confirmed that CoS_2 is a true semimetal that hosts Weyl fermions.

Superconducting properties of structurally related Ir–Te compounds ($IrTe_2$, Ir_3Te_8, and Ir_xTe_2) with different chemical doping and applied external pressure have recently been investigated in relation to their bonding and structural properties. These compounds undergo a major structural transition instead of progressive variations of the crystal lattice parameters. More freedom in crystal chemistry is offered in the ternary cobaltite compounds *TYX* (where *T* is a transition metal, *Y* is a pnictogen, and *X* is a chalcogen), most of which (over a hundred are known) crystalize in pyrite-type or closely related structures and contain bond anion pairs X_2, Y_2, or *XY*. The electronic or crystalline structure of cobaltites can be widely tuned by chemical substitution or external pressure. Investigating the interplay between crystal structure and electronic properties facilitates elucidation of the mechanism of superconductivity in pyrite-type materials.

Single crystals of $IrBi_{1-x}Te_{1+x}$ ($x \approx 0.2$), grown by the Bi-flux method [15], exhibit the pyrite-type structure (space group $Pa\bar{3}$, No. 205) with a refined lattice constant $a = 6.5004(3)$ Å. This is consistent with literature. The refinement of the atomic occupancy verifies that Bi is partially substituted by Te, resulting in the formula $IrBi_{0.79}Te_{1.21}$.

Upon substituting some of the Bi atoms in $IrBi_{0.79}Te_{1.21}$ with Te to achieve an actual composition $IrBi_{0.8}Te_{1.2}$, metallic behavior is observed (Figure 4a) [15], in contrast to the reported semiconducting behavior of IrBiTe. Furthermore, $IrBi_{0.8}Te_{1.2}$ demonstrates bulk superconductivity below 1.7 K (Figure 4a), which is further evidenced by the jump in specific heat capacity at T_c. Furthermore, the transition temperature shifts to lower temperatures with increasing magnetic field (Figure 4b).

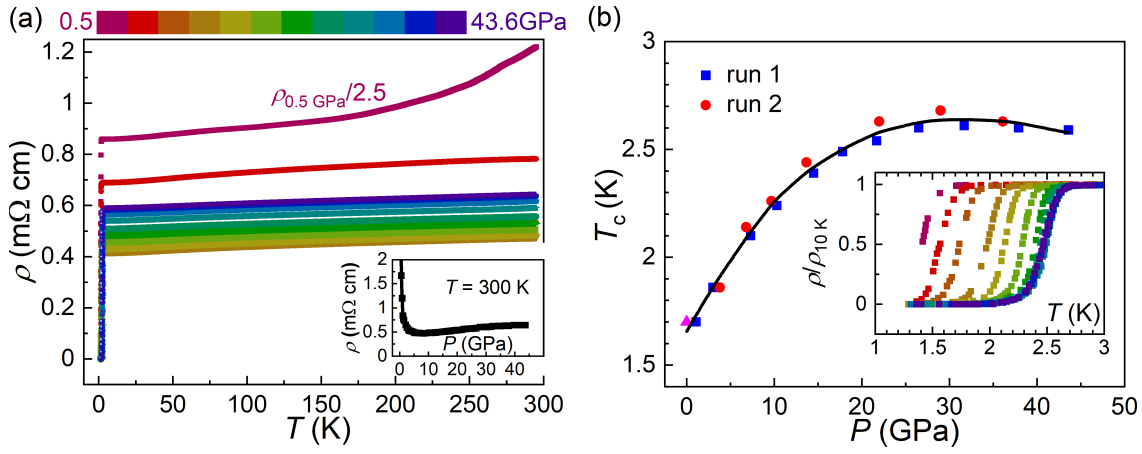

Fig. 5: Superconductivity of $IrBi_{0.8}Te_{1.2}$ at high pressure. (a) Temperature dependence of electrical resistivity down to T_{min} = 1.3 K under selected pressures. Inset: Pressure dependence of room-temperature resistivity up to 45 GPa. (b) Pressure dependence of T_c obtained from two experimental runs. Inset: Normalized resistivity below 3 K derived from the resistivity data in panel (a).

The application of external pressure enhances the superconducting transition temperature of $IrBi_{0.8}Te_{1.2}$ (Figure 5a). The highest T_c value (2.6 K) was achieved at a pressure of 26.5 GPa. With further compression, T_c decreases slightly, demonstrating a dome-shaped dependence on pressure (Figure 5b).

In the normal state, $IrBi_{0.8}Te_{1.2}$ displays metallic behavior up to the highest applied pressure. Hall-effect measurement revealed that application of pressure increases the carrier density, which plays a crucial role in the enhancement of superconductivity. Our studies on $IrBi_{0.8}Te_{1.2}$ suggest that the *TYX* cobaltite family of ternary compounds with pyrite structures is a good platform for studies of superconductivity by modifying the chemical composition or applying pressure.

Charge density wave transitions and superconductivity in CsV_3Sb_5 single crystals

Single-crystal CsV_3Sb_5 with characteristic kagome layers (see report **TQC_03_Feng**) of V-atoms in the crystal structure was grown via chemical vapor transport reactions by members of our group. These samples exhibited good crystal quality and chemical homogeneity, leading to extraordinarily small widths of both the charge density wave (Figure 6) and superconducting transitions. A remarkably low density of charged point defects was mirrored by a very weak upturn (Curie-law term) of magnetic susceptibility at low temperatures. These crystals have been used in several investigations (e.g. [16–19]) in collaborations with various other leading groups worldwide.

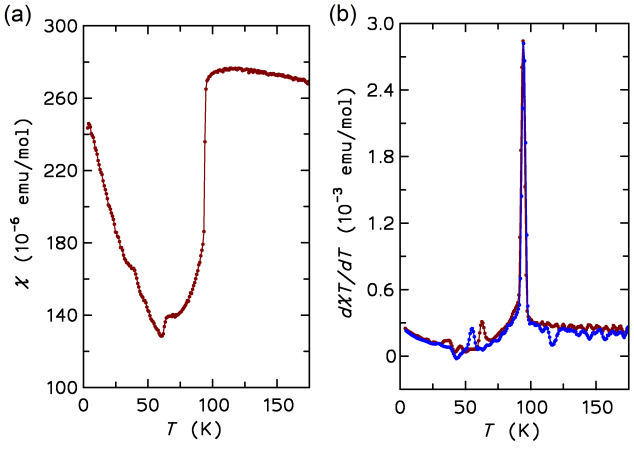

Fig. 6: (a) Magnetic susceptibility χ(T) of CsV_3Sb_5 along the crystallographic c direction and (b) derivative d(χT)/dT during warming (red) and cooling (blue). The temperature hysteresis of transitions between different charge density wave ordering patterns are visible. Unpublished data, cf. [16,18].

Outlook

While in the past years our superconductivity research was mostly centered around transition-metal chalcogenides under high pressure, now materials with layered but also clearly three-dimensional structures with flat bands have come into focus. Several compounds with kagome structure layers and rare-earth were already investigated by members of our group in this respect and we plan to extend research to some new Ni- and Cr-based systems and their high-pressure phases. It is well known that flat bands and van Hove singularities lead sequences of various ordered electronic states; however, the role of dispersion remains to be investigated in more detail.

We participate in the new SuperC consortium [20] devoted to the finding of new candidates for superconductors with high critical temperature by high-throughput DFT and phonon calculations combined with machine learning. Our group, besides the kagome materials, targets for the synthesis and investigation of Laves, AlB_2- and $ThCr_2Si_2$-type structure superconductors, which are of more three-dimensional character. In the last decade superconductivity has been discovered in compounds with large amounts of magnetic elements like Cr, Mn and Fe and we think there is potential to find more compound superconductors with such usually avoided elements at high pressure. Moreover, light-element compounds and their possibly superconducting phases at high pressure up to 100 GPa are of interest.

References

[1] *Superconductivity in $Cu_xBi_2Se_3$ and its implications for pairing in the undoped topological insulator, Y. S. Hor, A. J. Williams, J. G. Checkelsky, P. Roushan, J. Seo, Q. Xu, H. W. Zandbergen, A. Yazdani, N. P. Ong, R. J. Cava, Phys. Rev. Lett.* ***104*** *(2010) 057001, https://doi.org/10.1103/PhysRevLett.104.057001*

[2] *Pressure-induced unconventional superconducting phase in the topological insulator Bi_2Se_3, K. Kirshenbaum, P. S. Syers, A. P. Hope, N. P. Butch, J. R. Jeffries, S. T. Weir, J. J. Hamlin, M. B. Maple, Y. K. Vohra, J. Paglione, Phys. Rev. Lett.* ***111*** *(2013) 087001, https://doi.org/10.1103/PhysRevLett.111.087001*

[3] *Observation of unusual topological surface states in half-Heusler compounds LnPtBi (Ln = Lu, Y), Z. K. Liu, L. X. Yang, S. C. Wu, C. Shekhar, J. Jiang, H. F. Yang, Y. Zhang, S. K. Mo, Z. Hussain, B. Yan, C. Felser, Y. L. Chen, Nature Commun. 7 (2016) 12924, https://doi.org/10.1038/ncomms12924*

[4] *More than 50 Years after its Discovery in SiO_2 octahedral Coordination has also been established in SiS_2 at high Pressure, J. Evers, L. Mockl, G. Oehlinger, R. Koppe, H. Schnockel, O. Barkalov, S. Medvedev, P. Naumov, Inorg. Chem.* ***56*** *(2017) 372, https://doi.org/10.1021/acs.inorgchem.6b02294*

[5] *Pressure-induced transition to the collapsed tetragonal phase in $BaCr_2As_2$, P.G. Naumov, K. Filsinger, O.I. Barkalov, G.H. Fecher, S.A. Medvedev, C. Felser, Phys. Rev. B* ***95*** *(2017) 144106, https://doi.org/10.1103/PhysRevB.95.14410*

[6] *Pressure-induced metallization, transition to the pyrite-type structure, and superconductivity in palladium disulfide PdS_2, M.A. ElGhazali, P.G. Naumov, Q. Mu, V. Süß, A.O. Baskakov, C. Felser, S.A. Medvedev, Phys. Rev. B* ***100*** *(2019) 014507, https://doi.org/10.1103/PhysRevB.100.014507*

[7]* *Pressure-induced superconductivity and modification of Fermi surface in type-II Weyl semimetal $NbIrTe_4$, Q. Mu, F. Fan, H. Borrmann, W. Schnelle, Y. Sun, C. Felser, S. Medvedev, npj Quantum Materials* ***6*** *(2021) 55, https://doi.org/10.1038/s41535-021-00357-y*

[8] *Superconductivity in Weyl semimetal candidate $MoTe_2$, Y. Qi, P. Naumov, M. Ali, C. Rajamathi, O. Barkalov, M. Hanfland, S.-C. Wu, C. Shekhar, Y. Sun, V. Süß, M. Schmidt, U. Schwarz, E. Pippel, P. Werner, R. Hillebrand, T. Förster, E. Kampert, W. Schnelle, S. Parkin, R. Cava, C. Felser, B. Yan, S. Medvedev, Nature Commun. 7 (2016) 11038, https://doi.org/10.1038/s41535-021-00357-y*

[9]* *Spiral magnetism, spin flop, and pressure-induced ferromagnetism in the negative charge-transfer-gap insulator Sr_2FeO_4, P. Adler, M. Reehuis, N. Stüßer, S.A. Medvedev, M. Nicklas, D. C. Peets, J. Bertinshaw, C. K. Christensen, M. Etter, A. Hoser, L. Schröder, P. Merz, W. Schnelle, A. Schulz, Q. Mu, D. Bessas, A. Chumakov, M. Jansen, C. Felser, Phys. Rev. B* ***105*** *(2022) 054417, https://doi.org/10.1103/PhysRevB.105.054417*

[10]* *Interplay of structure and magnetism in $LuFe_4Ge_2$ tuned by hydrostatic pressure, M. O. Ajeesh, P. Materne, R.D. dos Reis, K. Weber, S. Dengre, R. Sarkar, R. Khasanov, I. Kraft, A. M. León, W. Bi, J. Zhao, E.E. Alp, S. Medvedev, V. Ksenofontov, H. Rosner, H. H. Klauss, C. Geibel, M. Nicklas, Phys. Rev. B* ***107*** *(2023) 125136, https://doi.org/10.1103/PhysRevB.107.125136*

[11] *Phase relationship and superconductivity in the Bi-rich part of the binary system Rh–Bi, F. Weitzer, W. Schnelle, R. Cardoso Gil, S. Hoffmann, R. Giedigkeit, Y. Grin, Calphad* ***33*** *(2009) 27, https://doi.org/10.1016/j.calphad.2008.07.016*

[12] *Discovery of a weak topological insulating state and van Hove singularity in triclinic $RhBi_2$, K. Lee, G. F. Lange, L.-L. Wang, B. Kuthanazhi, T. V. Trevisan, N. H. Jo, B. Schrunk, P. P. Orth, R.-J. Slager, P. C. Canfield, A. Kaminski, Nature Commun.* ***12*** *(2021) 1855, https://doi.org/10.1038/s41467-021-22136-w*

[13]* *Pressure-induced superconductivity in monoclinic $RhBi_2$, K.-Y. Ma, S. Roychowdhury, J. Noky, H. Borrmann, W. Schnelle, C. Shekhar, C. Felser, S. A. Medvedev, arXiv:2409.06358, (2024), https://doi.org/10.48550/arXiv.2409.06358*

[14] *Pressure-induced multiband superconductivity in pyrite $PtBi_2$ with perfect electron-hole compensation, X. Chen, D. Shao, C. Gu, Y. Zhou, C. An, Y. Zhou, X. Zhu, T. Chen, M. Tian, J. Sun, Z. Yang, Phys. Rev. Mater.* ***2*** *(2018) 054203, https://doi.org/10.1103/PhysRevMaterials.2.054203*

[15]* *Superconductivity in ternary pyrite-type compound $IrBi_{1-x}Te_{1+x}$ ($x \approx 0.2$) at ambient and high pressure, Q.-G. Mu, W. Schnelle, G.-W. Li, H. Borrmann, C. Felser, S. Medvedev, arXiv:2409.05649, (2024), https://doi.org/10.48550/arXiv.2409.05649*

[16]* *Temperature-driven reorganization of electronic order in CsV_3Sb_5, Q. Stahl, D. Chen, T. Ritschel, C. Shekhar, E. Sadrollahi, M. C. Rahn, O. Ivashko, M. v. Zimmermann, C. Felser, J. Geck, Phys. Rev. B* ***105*** *(2022) 195136, https://doi.org/10.1103/PhysRevB.105.195136*

[17]* *Three-dimensional Fermi surfaces from charge order in layered CsV_3Sb_5, X.-W. Huang, C.-Y. Guo, C. Putzke, M. Gutierrez-Amigo, Y. Sun, M. G. Vergniory, I. Errea, D. Chen, C. Felser, P. J. W. Moll, Phys. Rev. B* ***106*** *(2022) 064510, https://doi.org/10.1103/PhysRevB.106.064510*

[18]* *Charge density wave order and fluctuations above T_{CDW} and below superconducting T_c in the kagome metal CsV_3Sb_5, Q. Chen, D. Chen, W. Schnelle, C. Felser, B. D. Gaulin, Phys. Rev. Lett.* ***125*** *(2022) 056401, https://doi.org/10.1103/PhysRevLett.129.056401*

[19]* *High resolution polar Kerr effect studies of CsV_3Sb_5: Tests for time-reversal symmetry breaking below the charge-order transition, D. R. Saykin, C. Farhang, E. D. Kountz, D. Chen, B.R. Ortiz, C. Shekhar, C. Felser, S. D. Wilson, R. Thomale, J. Xia, A. Kapitulnik, Phys. Rev. Lett.* ***131*** *(2023) 016901, https://doi.org/10.1103/PhysRevLett.131.016901*

[20] *Room Temperature Superconductivity by 2033 research project, https://superc2033.com/*

[#] sergiy.medvediev@cpfs.mpg.de